Electronic Supplementary Information

On-surface coordination chemistry of planar molecular spin systems: Novel magnetochemical effects induced by axial ligands

Christian Wäckerlin[a,‡], Kartick Tarafder[b,‡], Dorota Siewert[a], Jan Girovsky[a], Tatjana Hählen[a], Cristian Iacovita[c], Armin Kleibert[d], Frithjof Nolting[d], Thomas A. Jung[a,*], Peter M. Oppeneer[b,*] & Nirmalya Ballav[e,*]

[a] Laboratory for Micro- and Nanotechnology, Paul Scherrer Institut, 5232 Villigen, Switzerland
[b] Department of Physics and Astronomy, Uppsala University, Box 516, S-751 20 Uppsala, Sweden
[c] Swiss Light Source, Paul Scherrer Institut, 5232 Villigen, Switzerland
[d] Department of Physics, University of Basel , 4056 Basel, Switzerland
[e] Department of Chemistry, Indian Institute of Science Education and Research (IISER), Pune - 411008, India
‡ Contributed equally.

Here, we provide supplementary information complementing the material presented in the article and supporting the therein presented conclusions and the experimental section (in Sec. 1). Specifically, STM data showing the morphology of the samples is presented (in Sec. 2), the XAS and XMCD of the ferromagnetic thin films are discussed (in Sec. 3) and the magnetochemical properties of CoOEP/Ni and CoPc/Ni are presented (in Sec. 4). The reduction/quenching of the XMCD signal in those two systems complements the conclusions discussed in the article. The temperature dependence of the XMCD/XAS ratio of native and NH_3 coordinated MnPc/Co is presented (in Sec. 5). A decrease in the exchange energy for the NH_3-MnPc complex is found in the experiment and in the DFT+U calculations, *i.e.* an influence of axial ligation onto the magnetic coupling. The reversibility of NO coordination with FeTPP/Ni is presented and compared with CoTPP/Ni and MnTPP/Co (in Sec. 6). The impact of the bonding configuration (physisorbed/chemisorbed) onto the spin states of FeP/Ni and NO-FeP/Ni is discussed on the basis of DFT+U calculations (in Sec. 7).

Table of Contents

1 Experimental section

The Ni and Co thin films of 20 monolayer thickness have been grown on Cu(001) single crystals, thereby producing ferromagnetic thin films with well defined magnetic shape-anisotropy in order to re-orient the sample magnetization with a limited external field[1,2]. CoTPP, FeTPPCl, MnTPPCl, MnPc, CoOEP and CoPc were evaporated (~0.7-0.9 ML) onto freshly prepared non-magnetized Ni and Co substrates kept at room temperature. Upon deposition of Fe(III)TPPCl and Mn(III)TPPCl onto Co and Ni substrates, Cl dissociates to form Fe(II)TPP and Mn(II)TPP[3,1].

We have used commercially available transition-metal compounds,. The purity of the 'as deposited' substance is generally higher due to the characteristics of the sublimation process. This is particularly true after thorough degassing at lower than sublimation temperatures. The molecules have been checked occasionally by sublimation with posterior chemical analysis and routinely with XPS [4]. The suppliers and purities (if available) are listed as follows:

- CoTPP, Co(II) tetraphenylporphyrin, Porphyrin Systems, Germany, 98 %
- CoPc, Co(II) phthalocyanine, Sigma-Aldrich, Switzerland
- CoOEP, Co(II) octaethylporphyrin, Sigma-Aldrich, Switzerland
- FeTPPCl, Fe(III) tetraphenylporphyrin chloride, Sigma-Aldrich, Switzerland
- MnTPPCl, Mn(III) tetraphenylporphyrin chloride, Porphyrin Systems, Germany, 98 %
- MnPc, Mn(II) phthalocyanine, Sigma-Aldrich, Switzerland

The quality of the substrates and the epitaxy of the monolayer and multilayer films was monitored by a quartz microbalance and verified in the XPS (monochromatic Al Kα excitation). The evaporation of the molecules was performed with home-built evaporators, the molecules were thoroughly degassed before sublimation, and the stochiometry after sublimation was checked by XPS. The evaporation rates were in the order of 0.5 to 0.25 ML/min, and the pressure during the evaporations was resided in the low 10^{-9} mbar regime. We would like to note that the used transition-metal compounds evaporate well and that XPS studies on multilayer films did not show the presence of impurities. The Co and Ni thin films were produced by electron beam evaporation, the Cu(001) single crystals were prepared by repeated cycles and Ar^+ ion sputtering and annealing. The cleanliness and morphology of the samples was checked by XPS and STM, respectively, c.f. refs. 1,2.

STM images were taken in the constant-current mode at room temperature using W tips. The ferromagnetic thin films were magnetized with an external magnetic field of ~150 mT along the respective easy axis of magnetization. The $L_{2,3}$-edges absorption spectra were recorded in total electron yield (TEY) mode in remanent magnetization of the substrate at the Surface/Interface: Microscopy (SIM) beamline of the Swiss Light Source (SLS)[5]. About 30 Langmuir (L) of NH_3 was dosed on the MnPc/Co system kept at ~80 K. Dosing of NO (~6000 L) on both CoTPP/Ni and MnTPP/Co systems was done at room

temperature while for the FeTPP/Ni system the temperature was kept at 100 K. All measurements were performed in UHV and a portable vacuum chamber was used for sample transfer[1,2].

For the DFT+U calculations, we have used the VASP full-potential plane-wave code[6] with a kinetic energy cut-off of 400 eV. The Perdew-Wang parametrization[7] of the DFT-generalized gradient approximation exchange-correlation functional was used. The Hubbard U and exchange constant J were taken to be 4 eV and 1 eV, respectively. We performed full geometric optimizations of the porphyrin molecules, including their distance and position on the surface, together with a full relaxation of the top substrate layers. Three atomic layers modeled the substrate. Reciprocal space sampling was performed using 2x2x2 Monkhorst-Pack k-points.

To manage computational efforts, we have carried out numerical calculations of the on-surface metallo-porphins (metal-P), *i.e.* without phenyl substitution[3,8–10]. The replacement of the phenyl end groups by hydrogen atoms might influence the magneto-chemical properties in the following ways. First, the phenyl end groups might induce a somewhat shorter or longer bonding distance of the metal-organic macrocycle to the substrate. This might affect the strength of the magnetic coupling of the central metal ion to the substrate. However, we do not expect that the magnetic coupling is changed thereby, for example, from parallel to anti-parallel coupling. It is also worthwhile to note that the current calculations (without phenyl end groups) reproduce fully the experimentally observed magneto-chemical couplings. Also, aspects of the NO or NH_3 bonding to the central metal ion will most likely not be affected. A second way in which the phenyl end groups might affect the coupling of the metal-organic molecule to the substrate could be through inducing a slight deformation of the macrocycle. Some forms of induced chirality have been observed by STM for metal-organic molecules on surfaces[11]. Such stronger chirality might affect the crystal electrical field at the central ion. An answer to the occurrence and possible importance of such deformations might be obtained from future precise STM measurements.

2 STM data

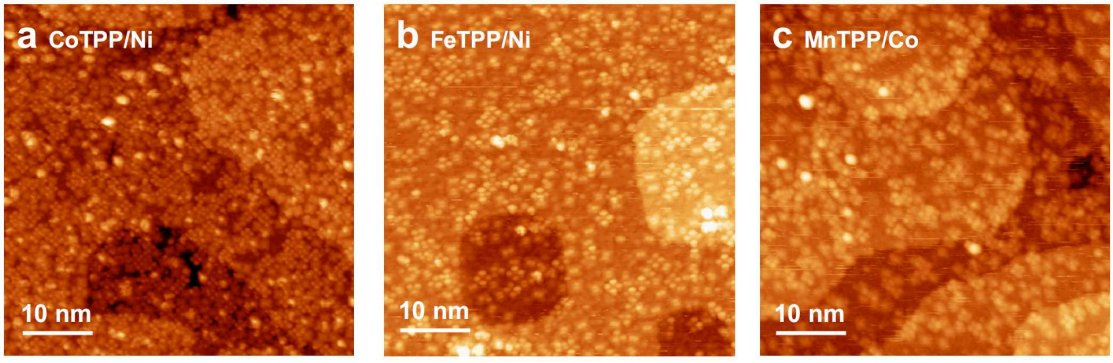

Fig. S1 STM images recorded on sub-monolayer coverages of the metallo-porphyrins on the ferromagnetic thin films: CoTPP/Ni (a), FeTPP/Ni (b) and MnTPP/Co (c).

In STM experiments performed at room-temperature (Fig. S1), we find that the metallo-porphyrins on the here studied ferromagnetic thin films (20 ML of Ni and 20 ML of Co on Cu(001)) do not self-assemble. The molecules are found in different adsorption geometries, *i.e.* conformations and orientations with respect to the substrate. Only a slight ordering between next neighbors is observed, mainly for FeTPP on Ni. The suppression of self-assembly at room temperature indicates a considerable interaction between the molecules and the substrate. This is in contrast to self-assembly as observed on less reactive substrates, *i.e.* oxygen-reconstructed Co/Cu(001)[1]. The STM tunneling parameters used in the shown STM data are: 1.05 V, 50 pA for Figs. 1b and S1a; -1.2 V, -60 pA for Fig. S1b; 1.25 V, 30 pA for Fig. S1c.

3 XAS and XMCD of the substrates

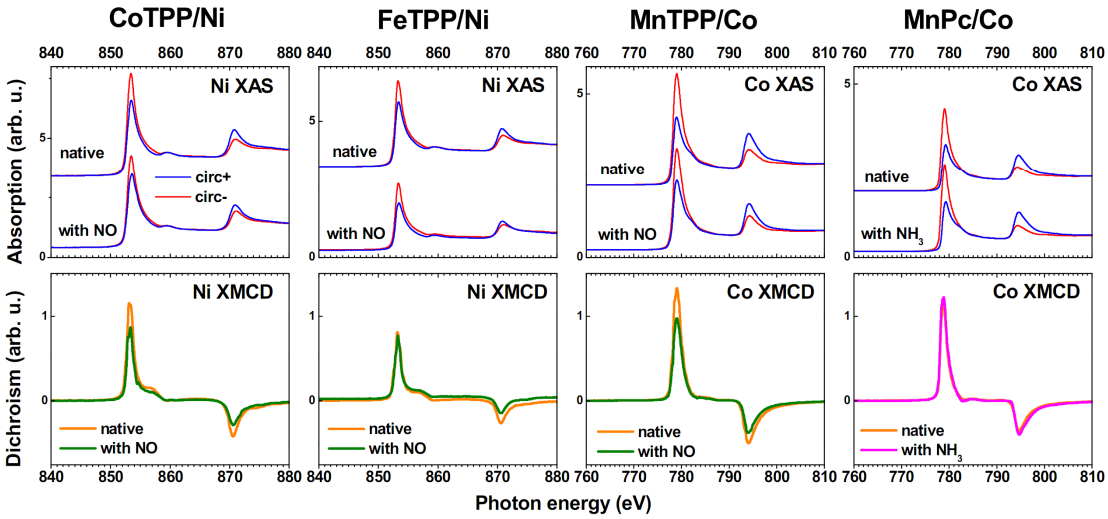

Fig. S2 XAS and XMCD of the substrates.

XMCD and XAS data of the substrates of the CoTPP/Ni, FeTPP/Ni, MnTPP/Co and MnPc/Co systems are shown in Fig. S2. Exposure with NO marginally affected the magnetization of the substrate, giving rise to a < 15 % reduction in the XMCD/XAS. When dosing NO/NH_3 onto the sample kept at ~100 K, *i.e.* as done for FeTPP/Ni and MnPc/Co no reduction in the XMCD/XAS signals is observed.

4 XAS and XMCD of CoOEP/Ni and CoPc/Ni

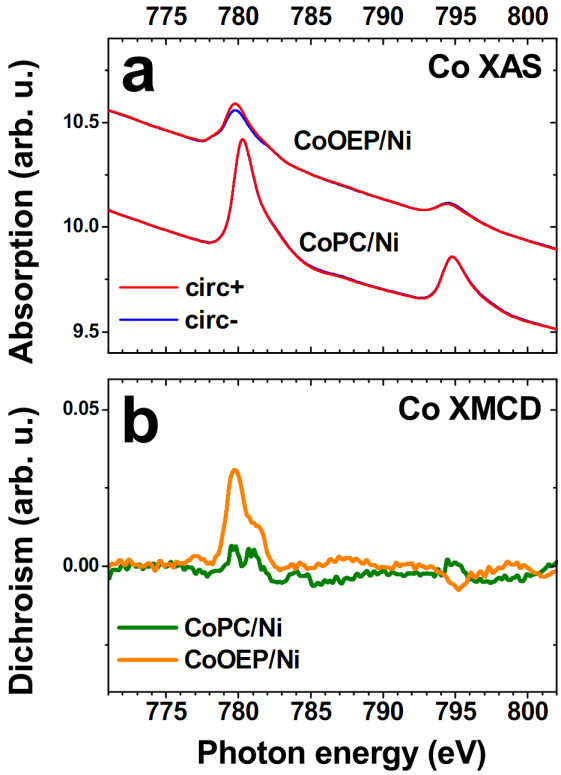

Fig. S3 XAS and XMCD of Co-phthalocyanine (CoPc) and Co-octaethylporphyrin (CoOEP) on Ni, measured at room temperature.

Performing a XAS and XMCD study of CoPc/Ni and CoOEP/Ni (Fig. S3) we find, in comparison to CoTPP/Ni (Figs. 2a1 and 2a2) with an XMCD/XAS ratio at the L_3-edge of ~23%, that the circular dichroism in CoOEP/Ni is reduced to ~15%, while CoPc/Ni shows only small remnant features in the circular dichroism, amounting to ~1.5% at the L_3 edge. Also, CoPc/Ni does not show the circular dichroism signal at the L_2 edge with opposite sign to that at the L_3 edge, as found in the other systems. Thus, the XMCD signal indicates the absence of a dipolar magnetic moment of CoPc on Ni.

In view of the literature[12–15] concerned with CoPc on ferromagnetic substrates and our DFT+U calculations, showing a reduction of the magnetic moment already in CoTPP/Ni (Figs. 3a and 3b), we tentatively explain the observed loss of the magnetic moment in CoPc and the observed reduction in CoOEP/Ni compared to CoTPP/Ni as a result of a strong hybridization of the half-filled d_z^2 orbital with substrate orbitals.

Note that, for CoPc/Au(111) where the absence of a Co XMCD is observed[16], too, this was explained in terms of a coherent superposition a d^7 and d^8 electronic states. This explanation could be considered in the present case as well, however keeping in mind the

decisive differences in the character of the Au and Ni substrates respectively: 6s vs. 3d bands at the Fermi level and diamagnetism vs. ferromagnetism.

5 Exchange coupling strength in MnPc/Co and NH_3-MnPc/Co

The temperature-dependence of the magnetization in MnPc was fitted with the Brillouin function[17]:

$$B_J(x) = \frac{2J+1}{2J}\coth\left(\frac{2J+1}{2J}x\right) - \frac{1}{2J}\coth\left(\frac{1}{2J}x\right)$$

In the model, the magnetization in the molecule μ_{mol} depends on the magnetization of the substrate μ_{sub}, the absolute temperature T and the exchange energy E_{ex}:

$$\mu_{mol} = \mu_{sub} B_J\left(\frac{E_{ex}}{k_B T}\right)$$

J is the total angular momentum and k_B the Boltzmann constant. For the fit, J was chosen in accordance with the DFT+U calculations to be 3/2 for MnPc and 2 for NH_3-MnPc. The exchange energies calculated from the fit vary only slightly with the choice of different values for J. The approach to extract the exchange energy is discussed in detail in Refs. [18,9].

The magnetic moment of Co was found to depend only weakly on the temperature (~5%)[18], and is therefore assumed to be constant.

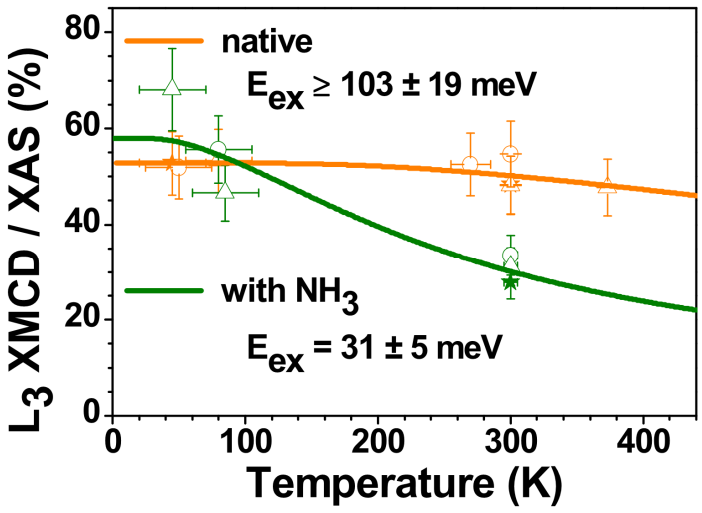

Fig. S4 Temperature dependence of the XMCD/XAS ratio of MnPc/Co before and after NH_3 exposure. The symbols (e.g. triangles, etc) mark different experimental runs.

The fit to the temperature dependence (Fig. S4) of MnPc/Co before NH_3 exposure, which yields a value of 103 meV, is to be seen as an estimate of a lower limit since the XMCD/XAS ratio was found to vary only slightly within the measured temperature range. In comparison, for FeOEP/Co, a high exchange energy of 70 meV was found [9].
After exposure to NH_3 with the sample kept at 70 K, and variation of the temperature, a significant temperature dependence of the XMCD/XAS ratio was found. The estimated exchange energy is ~31 meV.

Note, that the herein shown temperature dependence data before and after NH_3 exhibits significant scatter and high error bars mainly due to limitations in the control of the exact temperature, the coverage and the fact that at room temperature NH_3 was found to desorb slowly with a lifetime of a few hours.
The decrease of the exchange energy from ≥ 103 meV to 31 meV, is in *qualitative* agreement with the DFT+U calculations which yield values of 189 meV without NH_3 and 4 meV with NH_3.

6 Reversible coordination of NO on FeTPP/Ni and temperature dependence

Our XAS/XMCD experiments on FeTPP/Ni reveal that the coordination of NO onto FeTPP/Ni shows a very good reversibility by annealing to 260°C (Fig. S5).
The spin on Co of CoTPP/Ni is recovered by annealing to 340°C, a significantly higher temperature than for FeTPP/Ni, which opens up the possibility for structural changes on the reactive substrate as indicated by an incomplete (~70%) response to subsequent NO exposure. Notably, we found that NO coordination onto MnTPP/Co was not reversible in the experimental range up to 400°C.

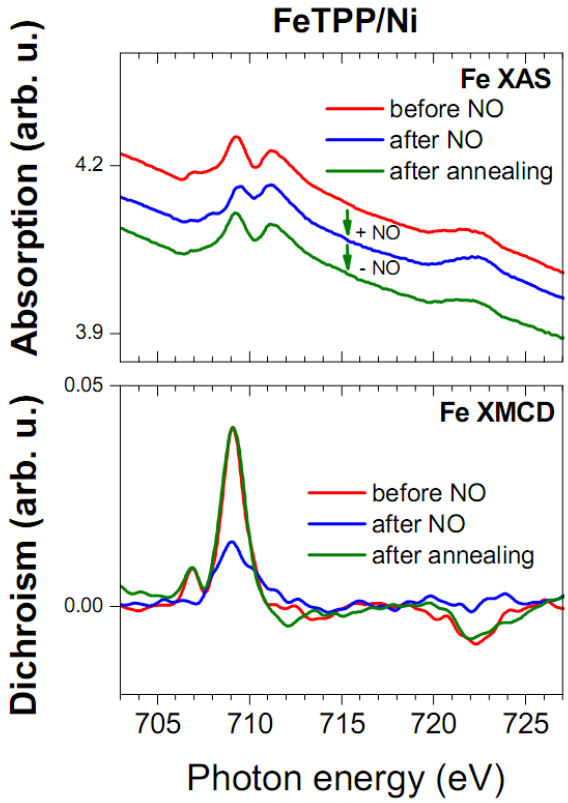

Fig. S5 XAS and XMCD of FeTPP/Ni for the native, NO-dosed and annealed system.

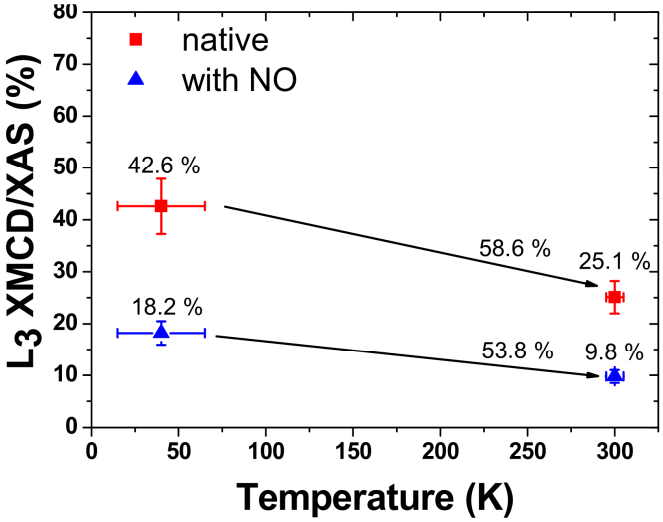

Fig. S6 Temperature dependence of the XMCD/XAS ratio of FeTPP/Ni before and after NO exposure. Compared to ~40K, the XMCD/XAS ratio of the room temperature data is reduced by 58.6 and 53.8 % respectively. This difference is within our error-bars, i.e. we do not observe a significant change of the exchange energy in FeTPP/Ni (+NO).

We have measured the XMCD/XAS ratio (Fig. S6) of FeTPP/Ni and NO-FeTPP/Ni at low temperature and at room temperature. However, the respective data taken at ~40 K and 300 K for FeTPP/Ni (before and after NO coordination) showed only a small difference in the Fe-XAS/XMCD ratio thereby suggesting that the magnetic exchange coupling strength was not significantly affected by the NO coordination. These observations are further confirmed by DFT+U calculations revealing an exchange energy of 114 meV for FeP/Ni and of 110 meV for NO-FeP/Ni.

7 FeP/Ni + NO: physisorption vs. chemisorption

In case of the intermediate-spin system FeTPP (S=1), the axial ligation with NO (S=1/2) is expected to lead to an S=1/2 state of NO-FeTPP if the surface is neglected (Fig. 1d). This is achieved by the unpaired spin of the NO in combination with the high ligand-field strength of NO imposing a low-spin electronic configuration in the nitrosyl complex.
The coordination of NO with FeTPP affecting the spin-state of Fe^{2+} ion is reflected by the Fe-XAS/XMCD spectra presented in Figs. 2c and 2d. Specifically, the vanishing of the Fe-XAS/XMCD shoulder peak at ~707.1 eV and diminishing of the main peak at ~709.2 eV is a signature of NO coordination. Importantly, the coordination of NO to FeTPP was found to be reversible by annealing to 260°C (*c.f.* Fig. S5).

In the DFT+U calculations we have considered both the *physisorbed* and *chemisorbed* FeP/Ni configuration (Fig. S7). In the latter adsorption configuration, the Fe ion distance to the top Ni layer is 2.19 Å and the Fe magnetic moment is 3.57 μ_B, *i.e.* a spin state between S=3/2 and S=2, with tiny magnetic moments existing on the N and C atoms in the molecule. Hence, the molecular spin has increased from S=1 for FeP in the gas phase. Ferromagnetic coupling of the FeP to the Ni is identified.

With NO, the molecule is significantly distorted and the Fe atom is pulled towards the NO leaving a distance of 2.55 Å to the surface. The Fe-NO bond angle is 169.5° and the Fe-NO bond length is 1.76 Å. Surprisingly, the magnetic moment of Fe is reduced only slightly to 3.49 μ_B. This small decrease in the Fe spin found in the DFT+U calculations for *chemisorbed* FeP on Ni is clearly not enough to explain the observed Fe-XMCD data obtained after NO exposure.

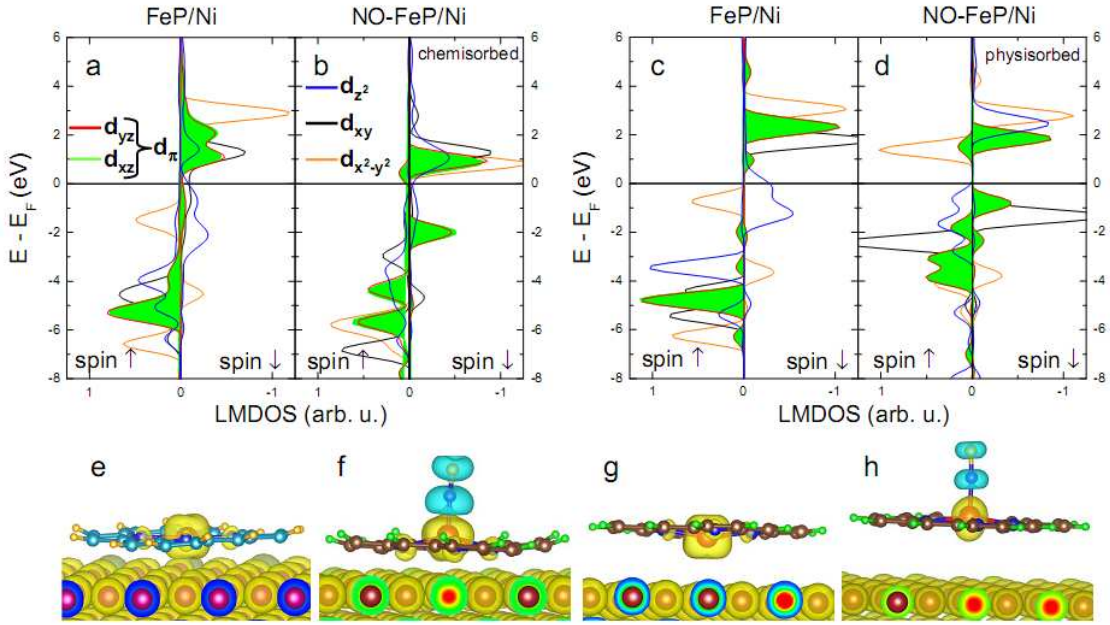

Fig. S7 Results of DFT+U calculations for FeP on Ni before and after NO coordination. Fe 3d orbital LMDOS for FeP/Ni (a) and NO-FeP/Ni (b) chemisorbed, and FeP/Ni (c) and NO-FeP/Ni (d) physisorbed on Co. Spin density isosurfaces for FeP/Ni and NO-FeP/Ni on Co, in chemisorbed (e&f) and physisorbed (g&h) configuration. Light yellow color denotes a spin density parallel to that of the Co substrate, light blue color an antiparallel spin density.

In the case of physisorbed FeP/Ni configuration, where the influence of the surface is weaker, the situation is different: the Fe magnetic moment is strongly reduced from 3.73 μ_B to 1.93 μ_B upon NO coordination (corresponding to a spin state close to S=1/2). Such a change in the molecular spin state is close to the expectations for the gas phase and can be seen as an effect of the strong ligand field of the NO-ligand resulting in an up-shift of the formerly singly occupied $d_{x^2-y^2}$ state which is almost completely unoccupied after NO coordination and a down-shift and occupation of the formerly singly occupied d_{xy} orbital. With NO, the distance from the surface is increased from 3.11 Å to 3.69 Å and Fe-NO bond length is 1.76 Å. Thus on the basis of our presented data, we prefer to assign the FeTPP/Ni system to be in rather physisorbed than chemisorbed configuration since the observed change in the XMCD in combination with the temperature dependence XAS/XMCD intensity ratio is consistent only with physisorption.

The calculated values are in good agreement with X-ray diffraction data on bulk NO-FeTPP, where a Fe-N-O angle of 149° and a Fe-N(NO) bond length of 1.72 Å is reported[19]. In this case, the NO-induced displacement of the Fe ion is 0.21 Å. This is clearly higher then in case of the NO-Co porphyrin bond.

In case of FeTPP/Ni, we find that the interaction with the substrate leads to an increase of the spin. Furthermore, we find that in contrast to CoTPP/Ni, NO exerts a significant

structural trans-effect. Not surprisingly, the coordination of NO (one unpaired electron) with d^6-Fe(II) (even number of electrons) does not result in a loss of the spin as for d^7-Co(II) (odd-number of electrons).

References

1. D. Chylarecka, C. Wäckerlin, T. K. Kim, K. Müller, F. Nolting, A. Kleibert, N. Ballav, and T. A. Jung, *J. Phys. Chem. Lett.*, 2010, **1**, 1408–1413.
2. C. Wäckerlin, D. Chylarecka, A. Kleibert, K. Müller, C. Iacovita, F. Nolting, T. A. Jung, and N. Ballav, *Nat. Commun.*, 2010, **1**, 61.
3. H. Wende, M. Bernien, J. Luo, C. Sorg, N. Ponpandian, J. Kurde, J. Miguel, M. Piantek, X. Xu, P. Eckhold, W. Kuch, K. Baberschke, P. M. Panchmatia, B. Sanyal, P. M. Oppeneer, and O. Eriksson, *Nat. Mater.*, 2007, **6**, 516–520.
4. P. Fesser, C. Iacovita, C. Wäckerlin, S. Vijayaraghavan, N. Ballav, K. Howes, J. Gisselbrecht, M. Crobu, C. Boudon, M. Stöhr, T. A. Jung, and F. Diederich, *Chem. Eur. J.*, 2011, **17**, 5246–5250.
5. U. Flechsig, F. Nolting, A. Fraile Rodríguez, J. Krempaský, C. Quitmann, T. Schmidt, S. Spielmann, D. Zimoch, R. Garrett, I. Gentle, K. Nugent, and S. Wilkins, *AIP Conf. Proc.*, 2010, **1234**, 319–322.
6. G. Kresse and J. Furthmüller, *Phys. Rev. B*, 1996, **54**, 11169–11186.
7. J. P. Perdew and Y. Wang, *Phys. Rev. B*, 1992, **45**, 13244–13249.
8. M. E. Ali, B. Sanyal, and P. M. Oppeneer, *J. Phys. Chem. C*, 2009, **113**, 14381–14383.
9. M. Bernien, J. Miguel, C. Weis, M. E. Ali, J. Kurde, B. Krumme, P. M. Panchmatia, B. Sanyal, M. Piantek, P. Srivastava, K. Baberschke, P. M. Oppeneer, O. Eriksson, W. Kuch, and H. Wende, *Phys. Rev. Lett.*, 2009, **102**, 047202.
10. P. M. Oppeneer, P. M. Panchmatia, B. Sanyal, O. Eriksson, and M. E. Ali, *Prog. Surf. Sci.*, 2009, **84**, 18–29.
11. A. Mugarza, R. Robles, C. Krull, R. Korytár, N. Lorente, and P. Gambardella, *Phys. Rev. B*, 2012, **85**.
12. C. Iacovita, M. Rastei, B. Heinrich, T. Brumme, J. Kortus, L. Limot, and J. Bucher, *Phys. Rev. Lett.*, 2008, **101**, 116602.
13. J. Brede, N. Atodiresei, S. Kuck, P. Lazić, V. Caciuc, Y. Morikawa, G. Hoffmann, S. Blügel, and R. Wiesendanger, *Phys. Rev. Lett.*, 2010, **105**, 047204.
14. E. Annese, J. Fujii, I. Vobornik, G. Panaccione, and G. Rossi, *Phys. Rev. B*, 2011, **84**, 174443.
15. S. Lach, A. Altenhof, K. Tarafder, F. Schmitt, M. E. Ali, M. Vogel, J. Sauther, P. M. Oppeneer, and C. Ziegler, *Adv. Funct. Mater.*, 2012, **22**, 989–997.
16. S. Stepanow, P. Miedema, A. Mugarza, G. Ceballos, P. Moras, J. Cezar, C. Carbone, F. de Groot, and P. Gambardella, *Phys. Rev. B*, 2011, **83**, 220401.
17. C. Kittel, *Introduction to solid state physics*, Wiley, New York, 7th ed., 1996.
18. M. Bernien, PhD Dissertation, Freie Universität Berlin, 2009.
19. W. R. Scheidt and M. E. Frisse, *J. Am. Chem. Soc.*, 1975, **97**, 17–21.